The force generated by biological membranes on a polymer rod and its response: Statics and dynamics

D. R. Daniels[a] and M. S. Turner
Department of Physics, University of Warwick, Coventry CV4 7AL, United Kingdom

(Received 14 April 2004; accepted 20 July 2004)

We propose a theory for the force exerted by a fluctuating membrane on a polymer rod tip. Using statistical mechanical methods, the expression for the generated force is written in terms of the distance of the rod tip from the membrane "frame." We apply the theory in calculating the stall force and membrane displacement required to cease the growth of a growing fiber induced by membrane fluctuations, as well as the membrane force and membrane displacement required for rod/fiber buckling. We also consider the dynamics of a growing fiber tip under the influence of a fluctuation-induced membrane force. We discuss the importance of our results in various biological contexts. Finally, we present a method to simultaneously extract both the rigidity of the semiflexible rod and the force applied by, e.g., the membrane from the measurements of the bending fluctuations of the rod. Such a measurement of the force would give information about the thermodynamics of the rod polymerization that involves the usual Brownian ratchet mechanism. © *2004 American Institute of Physics.* [DOI: 10.1063/1.1794551]

I. INTRODUCTION

It is often of considerable interest in biological contexts to consider the interactions between the flexible rods and membranes.[1–3] Given that these interactions often arise through biological membranes and rods[2,3] coming into close and sustained contact with each other (due to the packing constraints in a cell for example),[2,3] an interesting issue arises as to how to get some measure of the forces at work within enclosed biological cells.[4–11] In this paper, we consider the force exerted by a membrane on a growing fiber (see Fig. 1) that typically arises in many biological scenarios.[2,12–15] This fluctuating membrane force impinges heavily on the late-time dynamics of the fiber growth as found in "biological thermal ratchets",[4–10,16,17] as well as the overall stability[11] and possible buckling transitions[12–14] of a rod/membrane system as found in the polymerizing microtubules confined in vesicles[15] and membrane-enclosed fibers.[2,3]

Via careful consideration of both the statistical mechanics and dynamics, we are theoretically able, in this work, to account for the interaction between a fluctuating membrane and a fiber tip. Unlike previous works,[4–10,12–14,16,17] we are able to quantitatively calculate the force generated by a fluctuating membrane on a fiber tip via a "microscopic" model and derive the force generated as a function of the rod to the membrane distance. Previous works[4–10,12–14,16,17] often assumed or postulated a definite functional form (e.g., Hookean) for the membrane force as a function of the rod to the membrane distance, whereas in the work presented here, we explicitly derive the membrane force. Furthermore, using the approach outlined in this work and via a well-known[1,2] microscopic model for membrane fluctuations, we are also able to parameterize the strength of the membrane-induced force on a growing rod tip in terms of the membranes underlying "elastic constants." The consequences of our model for the thermodynamics and kinetics of a rod/membrane system will be discussed in further detail in the following sections, but firstly, we proceed to outline the theory that we are going to use to describe the fluctuating membrane.

II. THEORY

We parameterize the position R of our $L\times L$ membrane as follows:[1]

$$\mathrm{R}=x\hat{\mathrm{i}}+y\hat{\mathrm{j}}+u(x,y)\hat{\mathrm{k}}, \tag{1}$$

where $u(x,y)$ measures the deviation of our membrane from a local flatness, which we take to be the x-y plane. We also need to specify the boundary conditions at the edges of our finite-size membrane as $u(0,y)=0$, $u(L,y)=0$ for $0\leqslant y\leqslant L$, and $u(x,0)=0$, $u(x,L)=0$ for $0\leqslant x\leqslant L$. These boundary conditions, when taken together, ensure that the membrane behaves sensibly along its perimeter (i.e., at large distances) and cannot be arbitrarily translated along the $\hat{k}$ axis. The specification of these boundary conditions constitutes an appropriate "framing"[1] of our membrane. We assume throughout that the size of the frame is large enough such that all physical results obtained in this work are relatively insensitive to the shape of the frame boundary. Given the mentioned boundary conditions, we can write $u(x,y)$ in terms of the following discrete Fourier modes:

$$u(x,y)=\sum_{n=1}^{\infty}\sum_{m=1}^{\infty}u_{nm}\sin\frac{n\pi x}{L}\sin\frac{n\pi y}{L}. \tag{2}$$

For the purposes of this work, we will use the following harmonic free energy (see the Appendix for the discussion of when this formalism remains valid) for the displacement $u(x,y)$,:[1]

[a]Author to whom correspondence should be addressed. Electronic mail: d.r.daniels@warwick.ac.uk

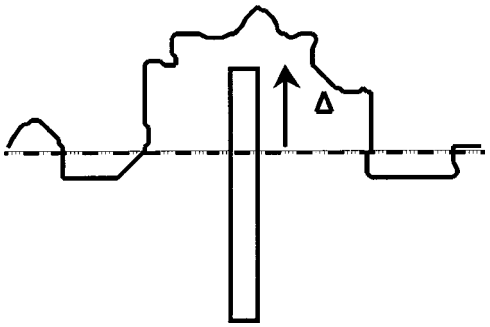

FIG. 1. Diagram of a fluctuating membrane interacting with a fiber tip. Δ denotes the height of the rod as measured from the membrane frame at $z=0$ (shown as a dashed horizontal line).

$$F_u=\frac{1}{2}\int_0^L dx\int_0^L dy(\kappa(\nabla_\perp^2 u)^2+\gamma(\nabla_\perp u)^2), \tag{3}$$

which contains a surface tension (γ) term as well as a curvature (κ) penalizing term. Note that the free energy in Eq. (3) is only really valid for relatively small displacements of u (see the Appendix for further details).

We now need to consider the form of the coupling between our membrane and the tip of a polymer rod lying along the $\hat{\mathrm{k}}$ axis (see Fig. 1). Note that we assume the rod tip to be ''pointlike,'' which is a valid approximation as long as the rod radius is less than the ''mesh size'' of the membrane (given by $\sim\sqrt{\kappa/\gamma}$). To begin with, we fix the midpoint fluctuations of our membrane to be fixed at some arbitrary value, z, as follows:

$$u(L/2,L/2)=z. \tag{4}$$

We incorporate this constraint into the calculation of the sum overall the membrane conformations, represented by our partition function Z_z, via the following relation:

$$Z_z=\int d\lambda Z_\lambda \exp(i\lambda z), \tag{5}$$

where Z_λ is defined as (unless otherwise stated, we take $k_BT=1$)

$$Z_\lambda=\int Du\exp(-i\lambda u(L/2,L/2)-F_u). \tag{6}$$

Carrying out the functional integral[18] in Eq. (6), we arrive at the following expression for Z_λ (normalized such that $Z_\lambda|_{\lambda=0}=1$).

$$Z_\lambda=\exp\left(-\frac{2\lambda^2}{\pi^2\gamma}\sum_{n=1}^{\infty}\sum_{m=1}^{\infty}\left(\frac{1}{K_{nm}}-\frac{1}{K_{nm}+\frac{\gamma L^2}{\pi^2\kappa}}\right)\right), \tag{7}$$

where we have defined $K_{nm}=(2n-1)^2+(2m-1)^2$. Unfortunately, the summations over n and m present in Eq. (7) do not lead to closed, convenient expressions. Therefore, for the purposes of this work and ease of use, we approximate the sums by integrals, enabling us to write

$$Z_\lambda=\exp\left(-\frac{\lambda^2}{8\pi\gamma}\ln\left(1+\frac{\gamma L^2}{\kappa\pi^2}\right)\right). \tag{8}$$

Now, carrying out a final integration over λ, we arrive at the desired expression for Z_z

$$Z_z=\exp(-Az^2), \tag{9}$$

where we have defined for convenience the constant A (which does however depend on the characteristic parameters of our membrane) as

$$A=\frac{2\pi\gamma}{\ln\left(1+\frac{\gamma\Omega}{\kappa\pi^2}\right)}, \tag{10}$$

where Ω is the area of the membrane frame (e.g., $\Omega=L^2$ in our case). Now, Z_z in Eq. (9) represents the partition function for the midpoint fluctuations of our membrane, fixed at some arbitrary value z. In order to complete the calculation of the partition function for our membrane, including the presence of the rod, we need to further integrate Z_z from the position of the tip of the rod, Δ, to ∞. In this way, we realize the physical constraint that we wish to impose; that the membrane midpoint must fluctuate entirely above the rod tip—and never below it. So we write (introducing a convenient normalization)

$$Z_\Delta=\frac{\int_\Delta^\infty dz Z_z}{\int_{-\infty}^{\infty}dz Z_z}, \tag{11}$$

where Δ is the position of the tip along the $\hat{\mathrm{k}}$ axis. Carrying out the integrals in Eq. (11), we end up with our final expression for Z_Δ [where erf(x) is the error function]

$$Z_\Delta=\frac{1}{2}(1-\mathrm{erf}(\sqrt{A}\Delta)). \tag{12}$$

From Eq. (12), we are now in a position to be able to calculate the force exerted by the membrane on the polymer rod tip as follows:

$$f_\Delta=-\frac{\partial\ln(Z_\Delta)}{\partial\Delta}=2\sqrt{\frac{A}{\pi}}\frac{\exp(-A\Delta^2)}{1-\mathrm{erf}(\sqrt{A}\Delta)}. \tag{13}$$

The force, as given by Eq. (13), is plotted in Fig. 2 against the membrane frame to the tip distance and possesses the following limits of interest (see also the Appendix):

$$\begin{aligned} &f_\Delta\to 2A\Delta \quad \text{as} \quad \Delta\to+\infty,\\ &f_\Delta\to 2\sqrt{\frac{A}{\pi}}+\frac{4}{\pi}A\Delta \quad \text{as} \quad \Delta\to 0,\\ &f_\Delta\to\sqrt{\frac{A}{\pi}}\exp(-A\Delta^2) \quad \text{as} \quad \Delta\to-\infty. \end{aligned} \tag{14}$$

From these limits and Fig. 2, we can discern the following behavior of our rod/membrane system. For large, positive Δ (i.e., when the rod tip strongly distorts the membrane upwards), the force generated by the membrane on the tip, f_Δ, becomes Hookean with a spring constant given by $\simeq 2A$. For small Δ, the force is again Hookean type (with a spring con-

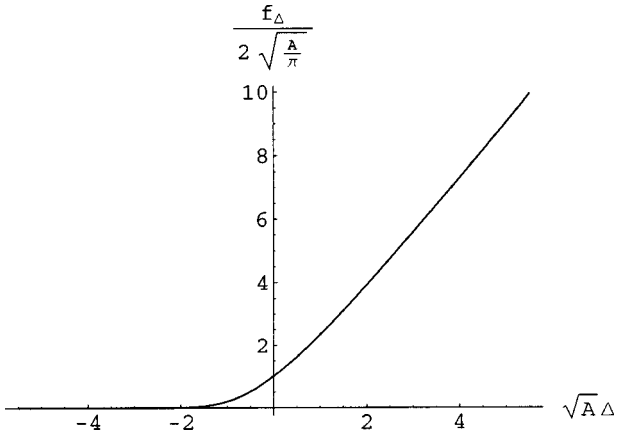

FIG. 2. Plot of the (normalized) force exerted by membrane $f_\Delta/2\sqrt{A/\pi}$ vs (normalized) distance of the tip from the membrane frame, $\sqrt{A}\Delta$.

stant now of $\simeq 4/\pi A$) but does not vanish as the rod tip approaches the membrane frame, but rather in this limit, f_Δ approaches the constant value of $2\sqrt{A/\pi}$. Lastly, when the rod tip is far away from the membrane frame (Δ large and negative), the force generated by the membrane decays away rapidly to zero, as one would expect. For comparison of the typical force magnitudes predicted by our model versus those found experimentally, see the Appendix.

We can also use the partition function Z_z for the midpoint fluctuations of our membrane, as given by Eq. (9), to calculate the average distance between the fiber tip and the fluctuating membrane, given that the midpoint fluctuations of the membrane must lie entirely above the rod tip—and never below it. So we are required to calculate with Z_z given by Eq. (9),

$$\langle z\rangle = \frac{\int_\Delta^\infty dz z Z_z}{\int_\Delta^\infty dz Z_z}. \tag{15}$$

Carrying out the integrals in Eq. (15), we arrive at the following expression for the average $\langle z\rangle$.

$$\langle z\rangle = \sqrt{\frac{1}{\pi A}}\frac{\exp(-A\Delta^2)}{1-\mathrm{erf}(\sqrt{A}\Delta)}. \tag{16}$$

As a by-product of this analysis and by combining Eqs. (16) and (13), we can obtain (as a useful consistency check) the force exerted by the membrane as a function of the average membrane displacement from zero, $\langle z\rangle$, as follows:

$$f_{\langle z\rangle} = 2A\langle z\rangle, \tag{17}$$

which can be seen to possess a simple Hookean functional form, as of course it should, since we began with a free-energy quadratic in the membrane displacement [Eq. (3)].

III. ROD GROWTH STALL FORCE

The dynamics of a growing fiber (as found in "Brownian Ratchets"[4–10,16] is governed by the rate of the monomer addition, $\alpha(0)=k_{\mathrm{on}}[M]$, and the rate of the monomer subtraction, $\beta(0)=k_{\mathrm{off}}$. Note that it is typically assumed that the rate of the monomer addition to the fiber depends on the concentration of the locally available monomers, M, whereas the rate of the monomer subtraction does not. Also note that in what follows, we assume that the available monomers are able to diffuse easily to the locally growing fiber tip [see, e.g., Eq. (4) for an example of when this may not be the case]. This assumption is tantamount to asserting that in this work, we take the rate-limiting step for the fiber growth to be the force exerted by our membrane and not the diffusion constant of the monomers.[4,17]

In the presence of a local force, f_Δ, acting on the growing rod tip and via the elementary Kramers transition rate theory,[4,5] it can be shown that the rate constants of the monomer (of typical size δ) addition and subtraction are modified in the following way:[4,5]

$$\begin{aligned}\alpha(f_\Delta) &= \alpha(0)\exp(-f_\Delta\delta),\\ \beta(f_\Delta) &= \beta(0).\end{aligned} \tag{18}$$

In Eq. (18), $f_\Delta\delta$ represents the work required to add one monomer of size δ to the growing tip, when the tip is at a distance Δ from the membrane frame. Note that it is usually assumed[4,5] that only the rate of the monomer addition is modified under the action of the local force, whereas the rate of the monomer subtraction remains unaffected by f_Δ.[4,5] For the purposes of this section, it is unnecessary to solve for the complete dynamics of the growing fiber, which we postponed to a later section. Since we are predominantly interested in this section in the stall force (i.e., the force required to halt the growth of the fiber), we only need to consider the equilibrium or steady-state behavior of the rod. Via elementary thermodynamical arguments,[4,5] it is straightforward to see that the rod growth stalls when the (new force-dependent) rate of the monomer addition equals the rate of the monomer subtraction, which implies the following result:[4,5]

$$\frac{\alpha(f_\Delta)}{\beta(f_\Delta)} = 1 \Rightarrow f_{\Delta\mathrm{stall}} = \frac{1}{\delta}\ln\left(\frac{\alpha(0)}{\beta(0)}\right). \tag{19}$$

Equation (19) expresses the simple idea that the rod growth stalls when the energy gain (or loss of entropy) produced by adding a monomer to the growing tip exactly balances the corresponding energy cost of doing the required work against the membrane. The following two limits are likely to be of most interest for stalling. If we focus on the small Δ, Hookean regime, we find that the onset of the stalling occurs when

$$\Delta_{\mathrm{stall}} \simeq \frac{\pi}{4A\delta}\ln\left(\frac{\alpha(0)}{\beta(0)}\right) - \frac{1}{2}\sqrt{\frac{\pi}{A}}. \tag{20}$$

On the other hand, if we focus on the large Δ, Hookean regime, we find that the onset of the stalling occurs when

$$\Delta_{\mathrm{stall}} \simeq \frac{1}{2A\delta}\ln\left(\frac{\alpha(0)}{\beta(0)}\right), \tag{21}$$

where A in both expressions is as given by Eq. (10). Using these limiting results, the corresponding value of the stall force in both the small and large Δ regimes can be straightforwardly obtained via inspection of the relevant limits given in Eq. (14) (see also the Appendix).

IV. ROD BUCKLING

Linear stability analysis[12–14] for a rod of length, L_{rod} and intrinsic stiffness, κ_{rod}, shows that a rod will buckle when the local force applied at the rod tip reaches the critical value of[12–14]

$$f_{\mathrm{buckle}} = \kappa_{\mathrm{rod}} \frac{\pi^2}{L_{\mathrm{rod}}^2}. \tag{22}$$

Equating the critical force, f_{buckle} of Eq. (22), with the force exerted by the membrane, given by f_Δ of Eq. (13), we can solve for Δ_{buckle}. The following two limits are likely to be of most interest for buckling. In particular, if we focus on the small Δ, Hookean regime, we find that the onset of the buckling occurs roughly when

$$\Delta_{\mathrm{buckle}} \simeq \frac{\kappa_{\mathrm{rod}} \pi^3}{4AL_{\mathrm{rod}}^2} - \frac{1}{2}\sqrt{\frac{\pi}{A}}. \tag{23}$$

On the other hand, if we focus on the large Δ, Hookean regime, we find that the onset of the buckling occurs when

$$\Delta_{\mathrm{buckle}} \simeq \frac{\kappa_{\mathrm{rod}} \pi^2}{2AL_{\mathrm{rod}}^2}, \tag{24}$$

where A in both expressions is again given by Eq. (10). Using these limiting results, the corresponding value of the buckling force, in both the small and large Δ regimes, can be straightforwardly obtained via inspection of the relevant limits given in Eq. (14) (see also the Appendix).

V. ROD GROWTH DYNAMICS

We now proceed to give an approximate ''mean-field-type'' description for the rod growth dynamics in close proximity to a fluctuating membrane. More complicated dynamical models can be found in the literature,[4–10,16] but for the purposes of this work, we prefer to use a simple and tractable model as possible, which nevertheless manages to accurately capture the underlying physics and furthermore renders the underlying physics as transparent as possible. Moreover, in the ''reaction-limited'' case as studied here, it can be shown [see, for example, Eq. (4)] that Eq. (25) can be derived from more complicated dynamical models. Thus, using the results of the previous sections, we can write down the (averaged over membrane fluctuations) dynamical equation obeyed by the fiber tip as[4–10,16]

$$\frac{d\Delta}{dt} = \delta(\alpha \exp(-f_\Delta \delta) - \beta). \tag{25}$$

From the right-hand side of Eq. (25), we can see that the rod growth comes to an end whenever the energy cost of adding a monomer becomes greater than the energy gain via entropy loss. Using Eq. (13) for f_Δ, we can solve Eq. (25) for $\Delta \equiv \Delta(t)$ numerically, as shown in Figs. 3 and 4.

Shown in Fig. 3 is the time evolution of the fiber-tip position at a fixed value of the rate constants for the monomer addition and subtraction $\alpha(0)/\beta(0)$, for three different values of $\sqrt{A\delta^2}$. The parameter $\sqrt{A\delta^2}$ roughly measures the ratio of the monomer size to the typical membrane fluctuation size $\sim\sqrt{\delta^2/\langle z^2\rangle}$, so that a high value of $\sqrt{A\delta^2}$ corresponds to a more rigid, hard-wall-type membrane, whereas a small value of $\sqrt{A\delta^2}$ corresponds to a more flexible, highly fluctuating surface. A typical value of $\sqrt{A\delta^2}\sim 0.4$ can be found experimentally (see the Appendix and Refs. 2, 4, 12, and 19). We can see from Fig. 3 that (for a given polymerization rate) the less flexible the membrane, the sooner the fiber growth begins to stall, whereas the more flexible the membrane, the later the fiber growth stalls. From Fig. 3, we can also see that the late-time, asymptotic value of $\Delta(t)$ is larger for the highly fluctuating membrane than that of the more rigid membrane. Reassuringly, all the plots shown in Fig. 3 converge for large negative fiber-tip membrane frame distances at earlytimes. One can understand these results qualitatively in terms of the underlying membrane fluctuations. The more highly fluctuating the membrane, the less the local, average force (or elastic constant) becomes on a rod tip, as the rod approaches the membrane surface. Furthermore, a highly fluctuating membrane is more likely on average to be able to accommodate the placement of a monomeric unit at the fiber tip than a rigid membrane, thus ameliorating the steric constraints, allowing the rod to grow longer.

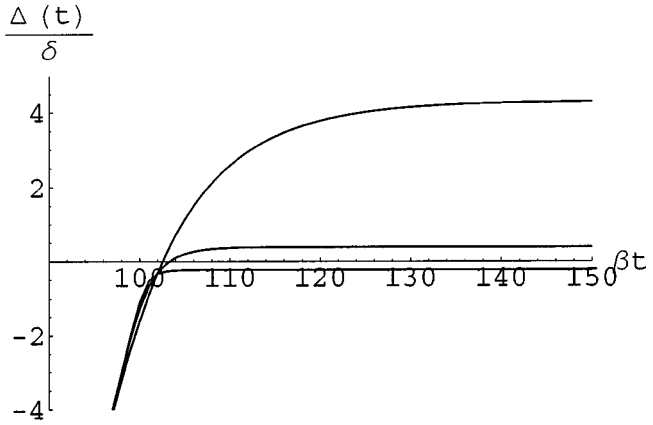

FIG. 3. Plot of the (normalized) fiber-tip position vs (normalized) time with $\alpha(0)/\beta(0)=2.0$. From top to bottom, $\sqrt{A\delta^2}=0.25$, 0.50, and 0.75.

Shown in Fig. 4 is the time evolution of the fiber-tip position at a fixed value of the membrane elastic constant $\sqrt{A\delta^2}$ for three different values of the ratio of the monomer

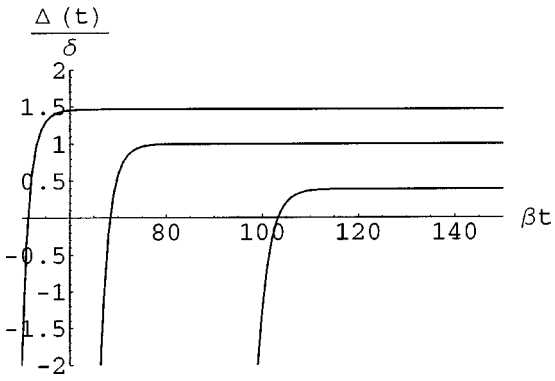

FIG. 4. Plot of the (normalized) fiber-tip position vs (normalized) time with $\sqrt{A\delta^2}=0.50$. From top to bottom, $\alpha(0)/\beta(0)=3.0$, 2.5, and 2.0.

addition to subtraction $\alpha(0)/\beta(0)$. A typical value of $\alpha(0)/\beta(0)\sim 2$ can be found experimentally.[4,5] From Fig. 4, one can easily see that increasing the rate of the monomer addition makes the fiber tip approach its late-time, asymptotic position more quickly and that, furthermore, this late-time, fiber-tip stall value increases as the rate of the monomer addition increases. These results can also be understood in terms of the membrane fluctuations as follows. Increasing the rate of the monomer addition implies that for the fiber tip to stall, a greater force needs to be exerted by the membrane. Now, if the membrane elastic constants are held fixed, then in order to produce the required stall force, the membrane must be deformed to a concomitantly higher degree, hence, the greater late-time, asymptotic value of the fiber-tip position.

VI. BENDING FLUCTUATIONS OF THE CONFINED SEMIFLEXIBLE FIBER

Motivated by recent experiments, we consider a single-living semiflexible rod or ''fiber'' in close proximity to a fluctuating membrane. Here, the term ''living'' merely denotes that the fiber can grow or shrink by the accretion of monomeric units. Such fibers could be, e.g., actin filaments, microtubules, or sickle hemoglobin fibers.[20] The geometries that we have in mind include a single fiber confined within a vesicle or a red blood cell. Under certain conditions, such living fibers have a tendency to grow in length. As usual, this is due to a free-energy imbalance between the monomers in solution and those in the fiber interior. When the end of a growing fiber starts to approach the cell membrane, it is subject to a longitudinal compressive confining force, f, the magnitude of which we have calculated earlier.

We parameterize the fluctuations of the fiber by way of the normal displacement $h(z)$ of the fiber from the z axis, chosen so as to be parallel to the end-to-end vector of the fiber. The displacement $h(z)$ is defined to be the normal displacement projected onto the x-z plane (say). Similar fluctuations would be apparent in projection onto the y-z plane, but these completely decouple from those in the x-z plane for the small amplitude bending fluctuations of interest here. Thus, the fiber projection is completely straight if $h=0$ is displaced upwards locally when $h>0$ and displaced downwards when $h<0$. The boundary conditions at the ends are $h(0)=h(L_{\rm rod})=0$. It can be shown that the mechanical energy of a fiber of length $L_{\rm rod}$ is well approximated by $H=H_x+H_y$ with

$$H_x=\int_0^{L_{\rm rod}} dz\left[\frac{\kappa_{\rm rod}}{2}\left(\frac{d^2h}{dz^2}\right)^2-\frac{f}{2}\left(\frac{dh}{dz}\right)^2\right], \tag{26}$$

provided that the fiber displacement everywhere is small $|h|/L_{\rm rod}\ll 1$. H_y is similar but is independent of the normal fiber displacement projected onto the x-z plane and may therefore be neglected in what follows. We simply observe that there will be exactly similar fluctuations in the y-z plane by symmetry. Here, $\kappa_{\rm rod}$ is, as before, the rigidity of the fiber and is simply a Hookean constant that relates squared curvature to bending energy. The force f can be shown to act as a Lagrange multiplier for excess length $\Delta L_{\rm rod}=1/2\int_0^{L_{\rm rod}}dz\,(dh/dz)^2$ for the small displacements of interest here. This force acts to do work in storing excess fiber length within $(0,L_{\rm rod})$.

Assuming that the gradients of the fiber ends remain unconstrained by the membrane, we proceed to consider the mode structure of the fluctuations by defining the Fourier pair as

$$h(z)=\sum_{n=1}^{\infty} h_n \sin\frac{n\pi z}{L_{\rm rod}}$$

and

$$h_n=\frac{2}{L_{\rm rod}}\int_0^{L_{\rm rod}} dz\,h(z)\sin\frac{n\pi z}{L_{\rm rod}}. \tag{27}$$

Thus, with $q_n\equiv n\pi/L_{\rm rod}$,

$$H_x=\frac{L_{\rm rod}}{4}\sum_{n=1}^{\infty} h_n^2(\kappa_{\rm rod}q_n^4-fq_n^2). \tag{28}$$

Equipartition of the energy applied to this Hamiltonian then yields

$$\langle h_n^2\rangle=\frac{2k_BT}{L_{\rm rod}(\kappa_{\rm rod}q_n^4-fq_n^2)}. \tag{29}$$

This expression correctly identifies the classical buckling force, $f_{\rm buckle}$, given in Eq. (22). The amplitude of the $n=1$ mode fluctuations diverge as $f\to f_{\rm buckle}$, and are unbounded for $f>f_{\rm buckle}$.

Fiber fluctuations and the applied force f and fiber rigidity $\kappa_{\rm rod}$

By measuring the mode spectrum of the fiber fluctuations, Eq. (29) can be used directly to calculate (fit for) the two unknowns f and $\kappa_{\rm rod}$. Thus, the fluctuations give independent information on, and in principle, determine both of these two unknown quantities. It has been previously reported how the measurements of the mean-squared displacement of the midpoint of freely suspended sickle fibers can be used to determine their rigidities,[21,22] there being no force ($f=0$) for freely suspended fibers. For such fibers, the rigidity was found to vary between the fibers, which could be interpreted as being due to the differences in the fiber thicknesses. A similar technique can be employed for the confined fibers as we will now show.

The projected fiber displacement at a distance z along the fiber is $h(z)$. The mean-squared value of this is

$$\langle h(z)^2\rangle=\sum_{n=1}^{\infty}\langle h_n^2\rangle\sin^2 q_nz=\frac{2k_BT}{L_{\rm rod}}\sum_{n=1}^{\infty}\frac{\sin^2 q_nz}{\kappa_{\rm rod}q_n^4-fq_n^2}. \tag{30}$$

Thus, the measurements of $\langle h(z)^2\rangle$ as few as two locations is enough to extract the two unknowns f and κ by any appropriate fitting procedure. In practice, the optimum information content is to be obtained by an analysis of as much of the mode structure as possible, i.e., as many n modes or equivalently z values as possible. However, for very rigid

fibers, the procedure of measuring the mean-squared spatial amplitudes at few locations can be nearly as efficient and is arguably more straightforward.

The important conclusion here is that we can measure the force f and hence obtain thermodynamic information about the system (by identifying the force as being due to a thermodynamic Brownian ratchet at a steady state) under conditions other than the special (marginal) case where the fiber is just starting to buckle. Thus, there is no need to fine tune the force or the chemical conditions. This gives, in principle, a new mechanism for mapping the thermodynamics of fiber assembly under all conditions, under which the fibers appear, provided the fiber fluctuations remain measurable. This is a very significant, if rather subtle, improvement over a technique that relies only on analyzing, e.g., fiber buckling.

VII. CONCLUSIONS

We have outlined the theory for the force exerted by a fluctuating membrane on a polymer rod tip using statistical mechanical methods. Unlike previous works, we do not assume or postulate a presubscribed functional form for the membrane force as a function of rod to the membrane distance.[4–10,16,18] Rather, in this work, we explicitly and quantitatively derive the membrane force acting on a fiber tip via a microscopic model and are furthermore able to parameterize the strength of this membrane-induced force in terms of the membranes underlying elastic constants. Using the approach given in this work, we were able to calculate the stall force required to cease the growth of a growing fiber induced by membrane fluctuations, as well as the membrane force needed for the rod/fiber buckling. We also studied the dynamics of a growing fiber tip under the action of a fluctuation-induced membrane force. The results obtained in this work are likely to have a direct and important bearing on the many relevant biological systems of interest, such as cells,[2–5,11,12] polymerizing microtubules[5,12,15] confined in vesicles, and membrane-enclosed fibers or rods.[2,3] The extension of the model presented in this work including the effects of spontaneous membrane curvature and/or membranes of spherical topology is left for future work. Finally, we have presented a method for the simultaneous extraction of the fiber rigidity and applied (membrane) force from the measurements of the bending fluctuations of the fiber.

ACKNOWLEDGMENT

This work was supported by the NIH with Grant No. HL 58512 from the National Heart Lung and Blood Institute.

APPENDIX: MODEL BREAKDOWN DISPLACEMENT AND FORCE

Our free energy for the membrane displacements, as given by Eq. (3), typically assumes[1,2] that the excess area produced by the membrane height fluctuations (over some reference base plane) is relatively small. This translates into the condition that our model breaks down[1,2] whenever $\nabla_\perp u \sim 1$, locally, anywhere over the entire membrane surface. In order to quantitatively predict when this breakdown occurs, we need to find the average local membrane shape, $\langle u(x,y)\rangle$, as a function of the in-plane membrane coordinates x and y, in the presence of the rod tip. Minimizing our free energy, Eq. (3), subject to the boundary conditions on the membrane edges and Eq. (4), we find that the shape of the membrane is given by

$$u(x,y)=\frac{z}{g(0,0)}g(x-L/2,y-L/2), \tag{A1}$$

where the "Green function" $g(x,y)$ satisfies

$$(-\gamma\nabla_\perp^2+\kappa\nabla_\perp^4)g(x,y)=\delta(x)\delta(y). \tag{A2}$$

In order to calculate the average membrane shape in the presence of the tip, we need to further average over the tip position such that

$$\langle u(x,y)\rangle=\frac{\langle z\rangle}{g(0,0)}g(x-L/2,y-L/2), \tag{A3}$$

where now $\langle z\rangle$ is given by Eq. (16) and is a function of the tip to the membrane frame distance Δ. Note that what we calculate here is the average displacement of the membrane, which is only nonzero due to the presence of the tip. In the absence of a tip, the average displacement of a membrane must strictly vanish. Using the rotational symmetry present, introducing $r=\sqrt{(x-L/2)^2+(y-L/2)^2}$ (such that the tip now sits at $r=0$), and converting to Fourier modes, we find that

$$g(r)=\int_{\pi/L}^{\infty}\frac{pdp}{2\pi}\frac{J_0(pr)}{\gamma p^2+\kappa p^4}, \tag{A4}$$

where $J_0(pr)$ is the familiar Bessel function of zeroth order, typically used in describing the membranes. We are now in a position to write $\langle\nabla_\perp u\rangle$ as

$$\langle\nabla_\perp u\rangle=\frac{\langle z\rangle}{g(0)}\frac{\partial g(r)}{\partial r}. \tag{A5}$$

It can be straightforwardly shown that $\langle\nabla_\perp u\rangle$ has its maximum value, $\langle\nabla_\perp u\rangle_{\max}$, when $r\sim\sqrt{\kappa/\gamma}$. Substituting this value of r into Eq. (35) and performing the integrals required, we get

$$\langle\nabla_\perp u\rangle_{\max}\simeq\frac{2}{5}\langle z\rangle\sqrt{\frac{\gamma}{\kappa}}\frac{1}{\ln\left(\frac{L}{\pi}\sqrt{\frac{\gamma}{\kappa}}\right)}. \tag{A6}$$

The condition for the breakdown of our model can now be finally expressed as occurring when the average membrane displacement reaches a maximum value, $\langle z\rangle_{\max}$ of

$$\langle z\rangle_{\max}\simeq\frac{5}{2}\sqrt{\frac{\kappa}{\gamma}}\ln\left(\frac{L}{\pi}\sqrt{\frac{\gamma}{\kappa}}\right). \tag{A7}$$

Using this result for $\langle z\rangle_{\max}$ along with Eq. (17), we can also calculate the maximum force, $f_{\max}$ capable of being generated in our model before it breaks down, which is given simply by

$$f_{\max}\simeq 5\pi\sqrt{\gamma\kappa}. \tag{A8}$$

Plugging in typical membrane values, as probed experimentally,[2,12,19] of $\kappa\sim 10^{-19}$ J, $\gamma\sim 10^{-4}$ J m^{-2}, and L

$\sim 10^{-6}$ m, we find that $\langle z \rangle_{max} \sim 200$ nm and $f_{max} \sim 50$ pN, which are consistent with typically observed experimental values for membrane displacements and forces as found in Refs. 2, 12, and 19. If we take the typical size of a monomer, δ, to be $\delta \sim 2$ nm,[4] then we can see that $\langle z \rangle_{max} \sim 100$ monomers. Thus, the theory outlined in this work is capable of providing a reasonable quantitative account of typical experimentally measured membrane forces and displacements.[2,12,19] Furthermore, the analysis carried out in this Appendix validates a posteriori, the initial use of a harmonic free energy for membrane displacements, which consequently also validates the resulting Hookean behavior of the force at relatively large membrane displacements.

[1] P. M. Chaikin and T. C. Lubensky, *Principles of Condensed Matter Physics* (Cambridge University Press, Cambridge, 2000).
[2] D. Boal, *Mechanics of the Cell* (Cambridge University Press, Cambridge, 2001).
[3] L. Mahadevan and P. Matsudaira, Science **288**, 95 (2000).
[4] C. S. Peskin *et al.*, Biophys. J. **65**, 316 (1993).
[5] M. Dogterom *et al.*, Appl. Phys. A: Mater. Sci. Process. **75**, 331 (2002).
[6] M. Dogterom and B. Yurke, Science **278**, 856 (1997).
[7] A. B. Kolomeisky and M. E. Fisher, Biophys. J. **80**, 149 (2001).
[8] A. Mogilner and G. Oster, Eur. Biophys. J. **28**, 235 (1999).
[9] S. van Doorn *et al.*, Eur. Biophys. J. **29**, 2 (2000).
[10] A. E. Carlsson, Phys. Rev. E **62**, 7082 (2000).
[11] E. Evans *et al.*, Biophys. J. **85**, 2342 (2003).
[12] D. K. Fygenson *et al.*, Phys. Rev. Lett. **79**, 4497 (1997).
[13] D. K. Fygenson *et al.*, Phys. Rev. E **55**, 850 (1997).
[14] E. Elbaum *et al.*, Phys. Rev. Lett. **76**, 4078 (1996).
[15] A. Desai and T. J. Mitchison, Annu. Rev. Cell Dev. Biol. **13**, 83 (1997).
[16] M. Dogterom and S. Leibler, Phys. Rev. Lett. **70**, 1347 (1988).
[17] D. J. Odde, Biophys. J. **73**, 88 (1997).
[18] H. Kleinert, *Path Integrals in Quantum Mechanics, Statistics, and Polymer Physics* (World Scientific, Singapore, 2004).
[19] A. R. Evans *et al.*, Phys. Rev. E **67**, 041907 (2003).
[20] W. A. Eaton and J. Hofrichter, Adv. Protein Chem. **40**, 63 (1990).
[21] J. C. Wang *et al.*, J. Mol. Biol. **315**, 601 (2002).
[22] M. S. Turner *et al.*, Langmuir **18**, 7182 (2002).